On the relationship of aeolian relief, micro-relief and wind direction with the concentration of dust aerosol in the near-surface layer

Malinovskaya E.A., Chkhetiani O.G., Maksimenkov L.O.

A.M. Obukhov Institute of Atmospheric Physics RAS

elen_am@inbox.ru

Vienna, 2021

Overview

1. Introduction
2. Empirical investigations
   - Geographical location and wind direction
   - Aeolean dune and inner layers
   - n-distribution functions
   - Mass concentration of microparticles distribution functions
3. Theoretical estimates
   - Micro-particle shaking off
   - Micro-particle chipping
   - Analytically derived distribution
   - Compare size distributions for micro-particle with estimates
4. Explanation of changing mass concentration
   - Changes mass concentration and wind direction
   - Compare size distributions for micro-particle with estimates
5. Conclusion

Introduction

The basic emission of particles of micron and submicron size is associated with the processes of collision and abrasion by interacting during saltation [1].

The larger particles have such mass that make short jumps or fell on the leeward slope during the avalanche collapse of sand from top and concentrate in the occurrence zone where there is no abrasion. Smaller fractions accumulate on the windward slope [2].

Saltation, secondary injection out of particles, and their rolling on the surface determines the emergence and growth of aeolian structures [3,4].

A kind of sorting occurs for the aeolian relief with a constant wind regime, which determines the zoning of the distribution of the intensity of aerosol generation due to different speed of abrasion.

Empirical investigations

Geographical location and wind direction

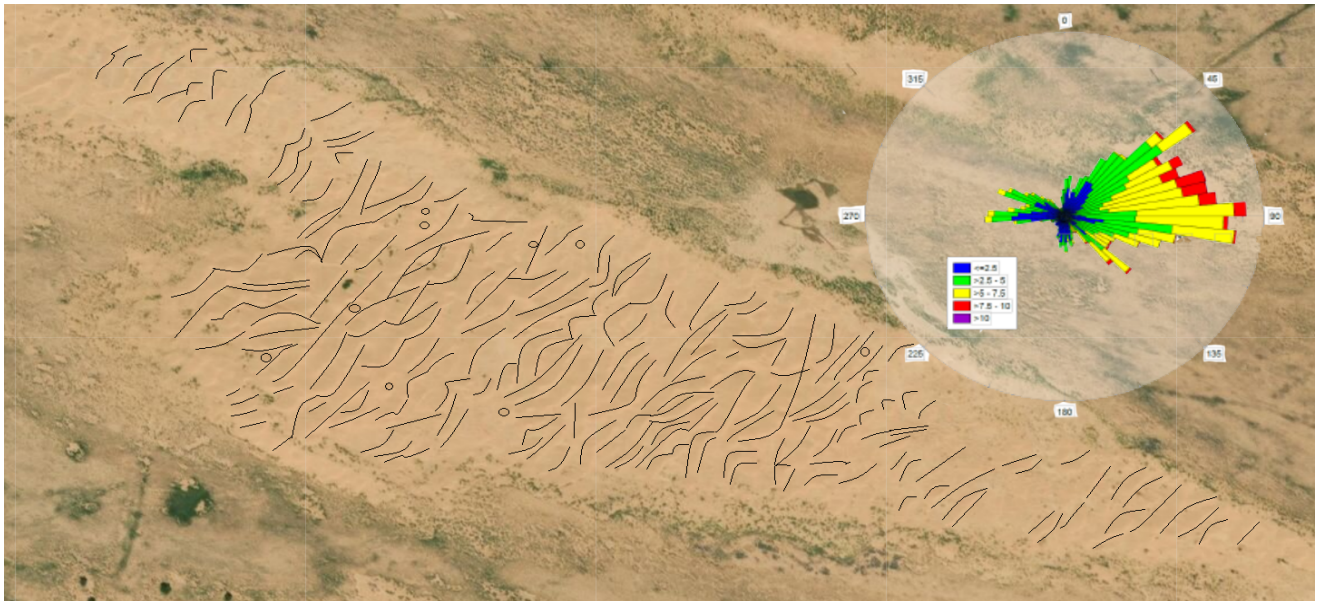


Figure 1: Geographical location of the mobile sands section with orientation to the sides of the world and orientation of the windward and leeward junction lines

Two wind directions are identified with respect to the lines of the tops of aeolian structures: frontal (ESE - east-south-east, E - east, WSW - west-south-west) and tangential (ENE - east-northeast, SW - southwest).

Selection of data

1. Air temperature 30-32°C
2. Wind speeds 3-6.5 m/s
3. In the evening

1. Investigations were made with using a selection of data from summer field measurements obtained
2. in the evening with close values of air temperature (30-32°C) and wind speeds (3-6.5 m/s)
3. on a perennial patch of unfixed sands approximately 1.5 km long and 200-300 m wide at 5 km west of Naryn Khuduk settlement (Russia, 2010-2020) [5,6].

Empirical investigations

Aeolean dune and inner layers

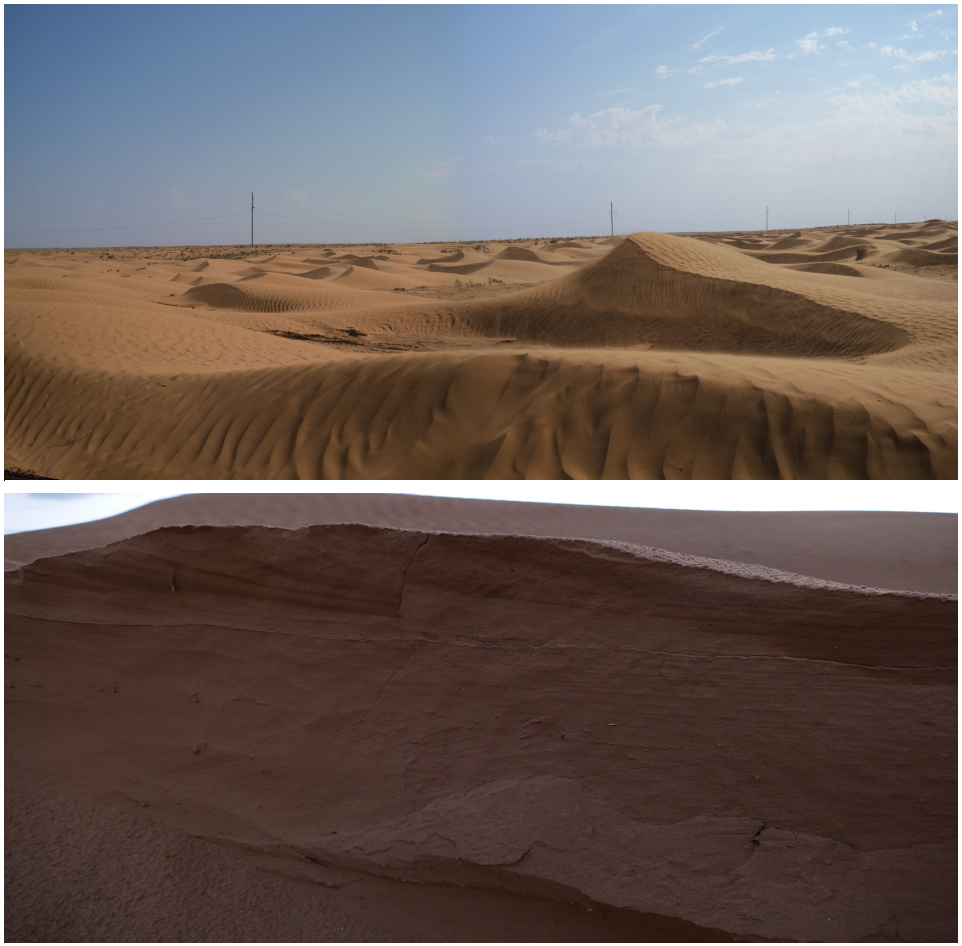


Figure 2: Panorama of the terrain and geological layers in the section of the aeolian structure, oblique layers

Aeolean structures

In the western part of the unfixed sand massif, the slopes are less gentle and there is a greater height difference than in the eastern part (fig. 2). The satellite image identifies the ridge top lines. The density of dune coverage is greater in the central part of the massif than on the eastern or western edges. Aeolian dune-type structures are 0.5 to 3 m high and ripples 1-5 cm high, with ridge spacing of 5-30 cm, depending on the location on the dune.

Layers into dune

The dune sand is represented by horizontal and parallel sloping layers of varying thickness 0.5-5 cm in section.

Empirical aerosol distribution functions

Based on the empirical aerosol distribution functions obtained for the above sample, a classification was made related to the wind direction in relation to the windward and leeward slope junction line: frontal and tangential.

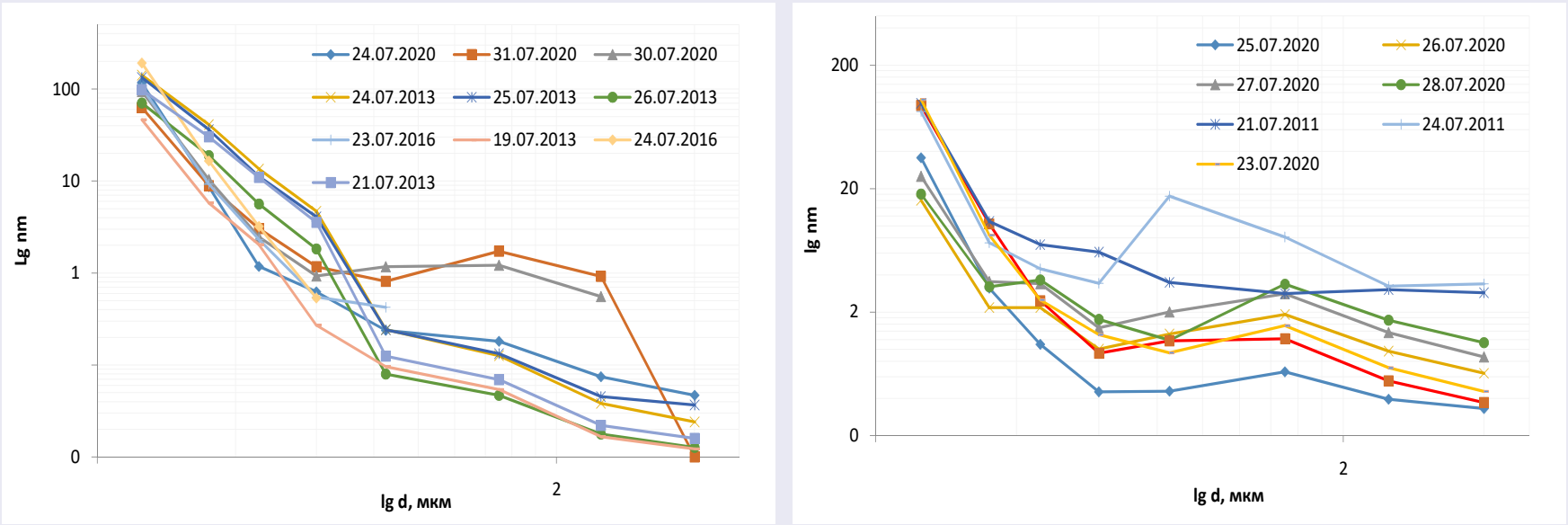


Figure 3: Micro-particle size distribution in frontal (left fig.) and tangential (right fig.) directions

Empirical investigations

Mass concentration of micro-particles distribution functions

Empirical aerosol mass concentration distribution functions

The data for the mass concentration of micro-particles Fig. 4(left) and Fig. 4(right) confirm the idea of wind energy expenditure during head-on and tangential movement.

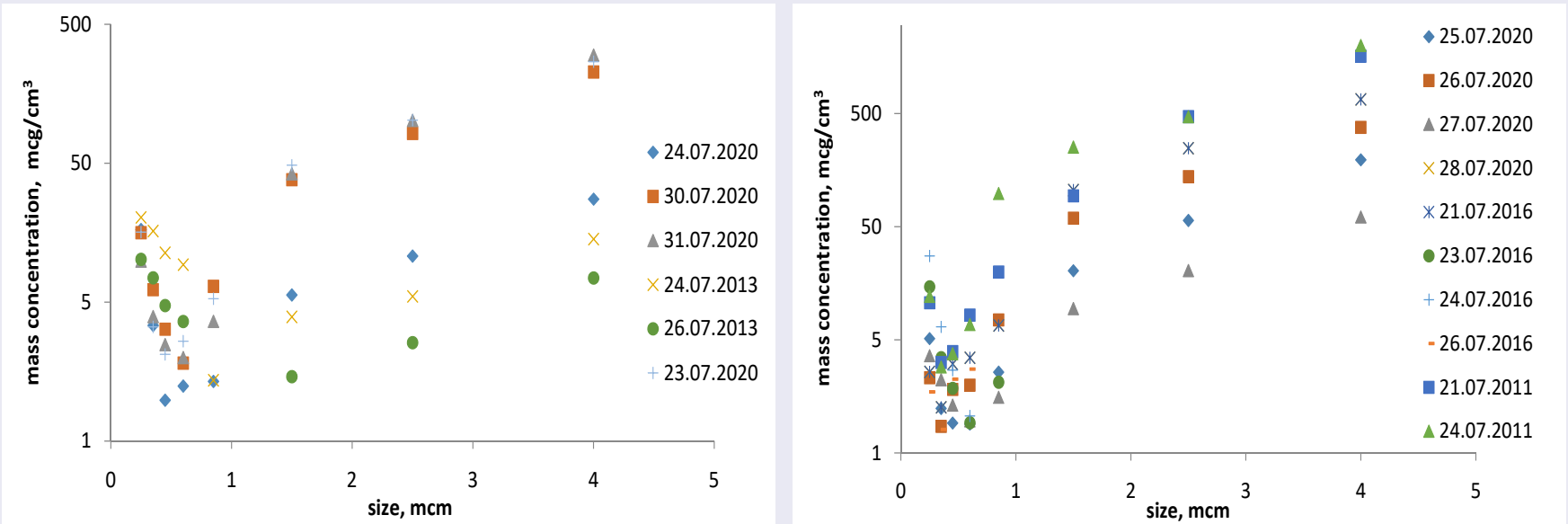


Figure 4: Micro-particle mass concentration distribution in frontal (left fig.) and tangential (right fig.) directions

Theoretical estimates

Micro-particle shaking off

Forces

Single micro-particles are attached to the surface of large particles, held together by Van der Waals and electrostatic forces. They are characterised by an inverse proportion to the size of the gap between the particle surfaces δ and a direct proportion to their radius r [7]: $\frac{r}{\delta}$. Generation of aerosol by bouncing particles as they fall onto the surface depends on the pressure force on the surface F_p, determined by the change in momentum [8]:

$$F_p = \frac{\rho_p \pi\, r^3 u^2}{\delta}, \qquad (1)$$

δ is the distance between the surfaces of the interacting particles, ρ_p is the density of the particle material, u is the velocity of the falling particles, r is the radius of the particles.

Estimates for size distribution

$$r = \frac{1}{r_\mu} \frac{\delta C_a}{\rho_p \pi\, u^2 \left(1 - \cos\alpha\right) \zeta_d}, \qquad (2)$$

$$n_{\mu 1} = \left[\frac{\delta\, C_a}{\rho_p \pi\, r_\mu^2 u^2 \left(1 - \cos\alpha\right) \zeta_d} \right]^2. \qquad (3)$$

The size of the flaked micro-particles is inversely proportional to the radius of the moving particles $r_\mu \sim \frac{1}{r}$. The number of micro-particles that can be chipped is inversely proportional to their radius to the power of 1/4: $n_\mu \sim \frac{1}{(r_\mu)^4}$.

Theoretical estimates

Micro-particle chipping

Threshold tensile strength for micro-elements

The strength of a material under various influences is determined by its elastic properties, i.e. the strength of the influence determines the size of the elements to be splintered. The value of the tensile strength is determined by the ratio of the impact force to the area $W = \frac{F}{s_\mu}$, and the tensile strength for quartz W is a known value (4.0 MPa). Increasing the pressure force on the surface as the particle falls or slips increases the number of splinters. The size of splintering particles is proportional to the root of the applied force: $r_\mu \sim \sqrt{F_P}$ [9]

Estimates for size distribution

$$r = \sqrt[3]{\frac{W r_\mu^2}{(1-\cos\alpha)\,\zeta_d}\,\frac{\delta}{\rho_p \pi u^2}} \tag{4}$$

There is a relationship between the radius of the moving particles and the size of the fractions to be splintered, as follows: $r \sim r_\mu^{2/3}$. Then for the number of particles that can be splintered we get:

$$n_{\mu 1} = \sqrt[3]{\frac{W}{(1-\cos\alpha)\,\zeta_d r_\mu^4}\,\frac{\delta}{\rho_p \pi u^2}}, \tag{5}$$

that is, $n_{\mu 1}$ is inversely proportional to the particle radius of the micro-particles r_μ to the power 4/3: $n_\mu \sim \frac{1}{(r_\mu)^{-4/3}}$.

Theoretical estimates

Analytically derived distribution

Threshold tensile strength for micro-elements

Desert particle sizes are characterized by a log-normal law for the size distribution of surface particles [10]]:

$$f(x) = \frac{0,43429}{\sigma_{\lg x} x \sqrt{2\pi}} \exp\left[-\frac{(\lg x - \lg x_0)^2}{2\sigma^2_{\lg x}}\right], \quad (6)$$

. Here x is the particle size, μm; x_0 – the average geometric size of the sand particle, μm; $\sigma_{\lg x}$ - is the standard deviation for logarithms of particle sizes.

Estimates for size distribution

We obtain relations linking the sizes of particles and micro-particles With using (3) and (5) of the form:

$$n_\mu = \begin{cases} A_1 r_\mu^{-4} f(r), r_\mu < r_{\mu 0} \\ A_2 r_\mu^{-4/3} f(r), r_\mu > r_{\mu 0} \end{cases}, \quad (7)$$

. Here $A_1 = \left[\frac{\delta C_a}{\rho_p \pi u^2 (1-\cos\alpha)\zeta_d}\right]^2$,

$A_2 = \sqrt[3]{\frac{W}{(1-\cos\alpha)\zeta_d} \frac{\delta}{\rho_p \pi u^2}}$

Estimates for size distribution

The appearance of the distribution (7) for the number of flaked and chipped particles varies with the parameters: windward velocity of massive particles u_d, deposition velocity of the flaked particles u_s, fraction of momentum transfer by micro-particles ζ_d during fall and others.

Theoretical estimates

Compare size distributions for micro-particle with estimates

For the selected days with the frontal (Fig.12) wind directions

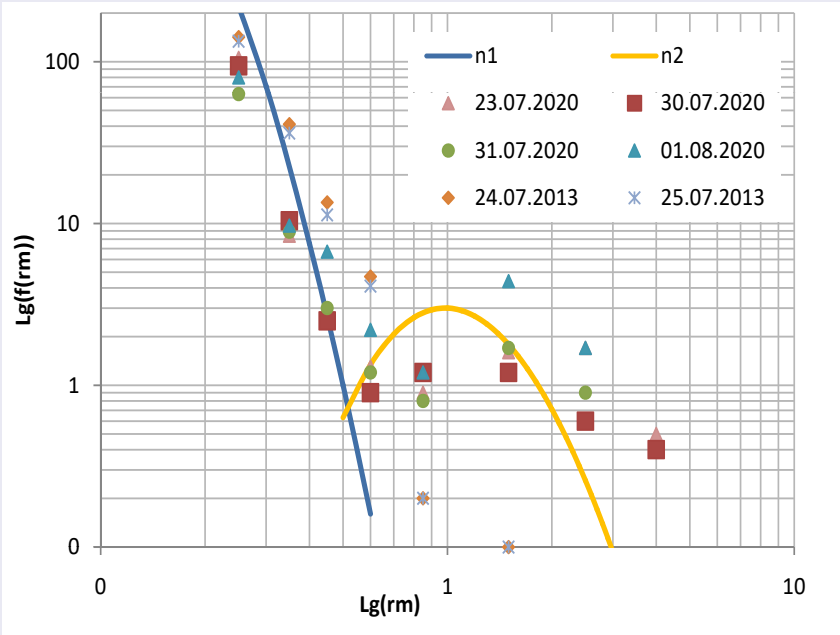


Figure 5: Micro-particle size distribution for the frontal wind direction calculated by (7) ($\alpha = 40^\circ, \zeta_d = 0.1$, splinter fraction 0,1)

For the selected days with tangential (Fig.6) wind directions

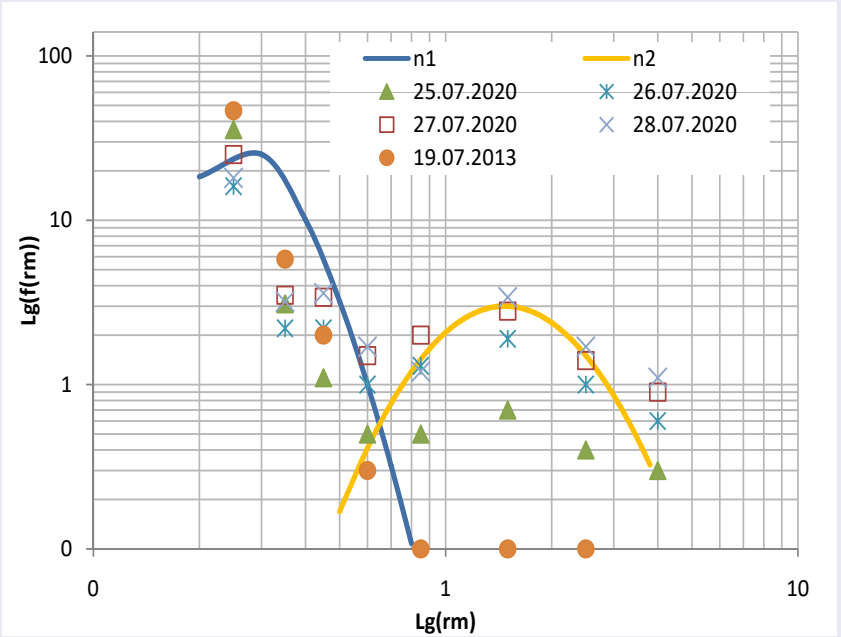
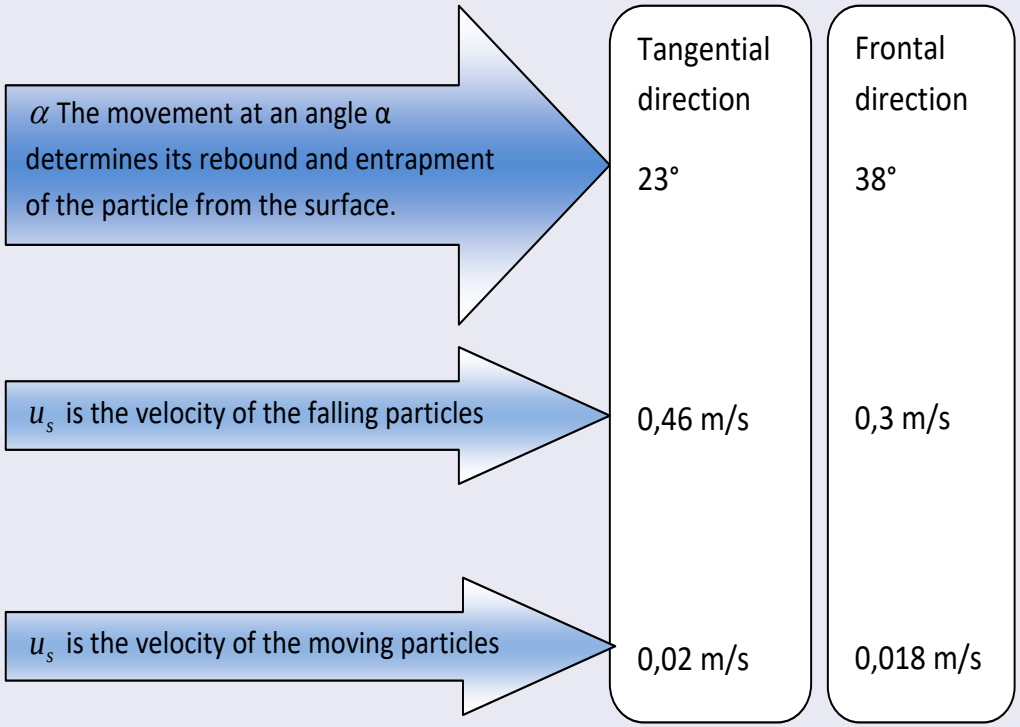


Figure 6: Micro-particle size distribution for the tangential wind direction calculated by (7) ($\alpha = 20^\circ, \zeta_d = 0.1$,splinter fraction 1)

Theoretical estimates

Compare size distributions for micro-particle with estimates

Determination of input parameters for distribution curves



For the selected days with tangential (Fig.6) wind directions

The theoretically obtained distribution relation is compared with measured data after normalisation.
The greatest effect when the wind direction changes from windward to tangential is due to a relative decrease in the velocity of falling particles on the surface and an increase in the velocity of rolling or moving massive particles down the windward slope.
The angle of incidence for the tangential direction is chosen less than that for the frontal.

Visual observations

Jets from the top of dunes in days with wet sand in down layers

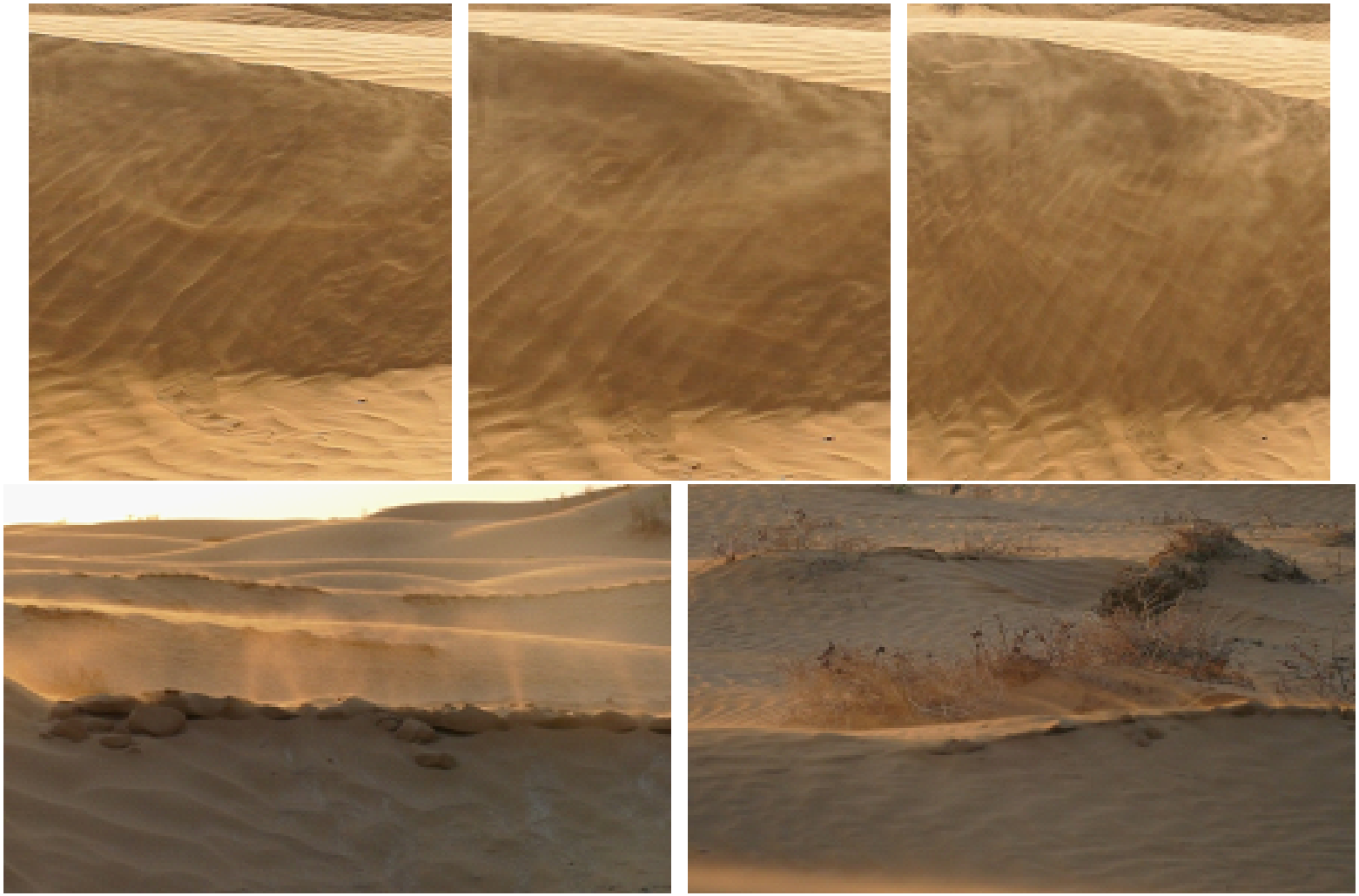


Figure 7: Jets from the top and swirling flow parallel to the surface plane on the leeward slope

Explanation of changing mass concentration

Changes mass concentration and wind direction

Table 1: Average data for selected days with close temperature and wind speed values between 17:00 and 20:00

	Wind direction	γ, $^\circ$	T, $^\circ C$	U, m/s	m_μ, $\mu g/cm^3$
28.07.20	60% NE NE+ENE	0-10	30.1	7.3	490.9
23.07.20	53% W, 27% WSW	40-50	31.1	5.5	449.0
25.07.20	83% ENE от NE+ENE	40-50	32.0	6.5	282.9
26.07.20	92% ENE от NE+ENE	40-50	31.8	6.4	590.9
27.07.20	57% ENE от NE+ENE	40-50	30.7	6.2	100.4
21.07.11	85% ESE от SE+ESE	70-80	36.0	7.6	2275.3
24.07.11	74% ESE от SE+ESE	70-80	30.5	7.3	2840.8
30.07.20	81% ESE от E+ESE	70-80	32.0	6.1	380.2
31.07.20	53% ESE от E+ESE	70-80	30.3	6.8	269.1

Notes to the table. ENE - east-north-east, NE - north-east, E - east, SE - south-east, ESE - east-south-east, W - west, WSW - west-south-west. γ is the angle of the wind line to the slope top line, T is the air temperature, U is the wind velocity, τ is the average value of the time interval between snowfall amplification, m_μ is the mass concentration of particles of 0.2-5 μ m

Marks

The mass concentration of dusty aerosol on days with a tangential wind direction is generally higher. On some days, significantly smaller ones are noted for the tangential direction.

Explanation of changing mass concentration

The decrease correlates with the micro-ripple event

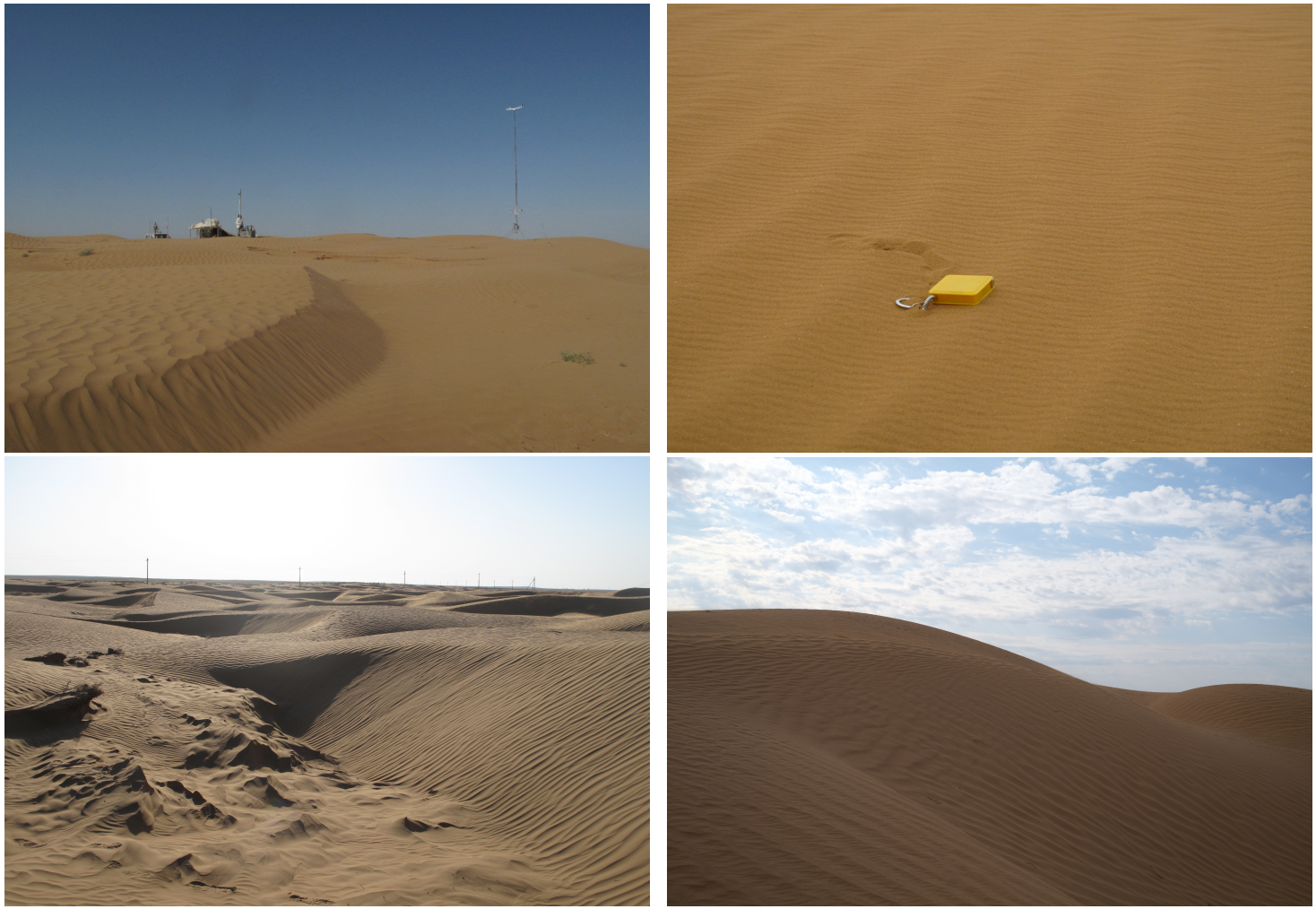


Figure 8: Micro-ripples in days with less concentration of dust aerosol: 28.07.20, 28.07.13, 20.07.11, 19.07.10

Conclusion

1. Estimates of pressure force for two variants of particle motion showed that the fine fraction is mainly generated when massive particles move near the surface without hopping. This motion causes shaking off of electrostatically adhered micro-particles to the surface of large particles. Saltating affects the breaking away of the larger aerosol fraction because its size is proportional to the force of the impact, and the falling velocity of the saltating particles is greater than that of the particles rolling at the surface.
2. Theoretical estimates of the size distribution of the number of micro-particles generated during shaking and fragmentation are proposed with using representations of empirical data and analytical estimates for threshold velocities. The micro-particle size distribution is defined by a piecewise defined function with two peaks. The ranges of generated micro-particles of fine and coarse fraction are different for tangential and frontal wind directions. Therefore it is possible to estimate the prevalence of one or another type of generation by the character of micro-particle size distribution.
3. Splashing effect appears in the frontal wind direction due to surface geometry of aeolian structures and characteristic angles of incidence of tangential particles. The process of particle transport is intensified on windward slope , secondary generation processes are more active, more layers are involved in transport process and there is more variety of generated particle sizes. The process of entrainment and transport is slowed down by elements of secondary aeolian ripple-type structures. There is its growth, slow renewal of layer composition due to capture of layers between ripple elements.

References

1. Houser C.A., Nickling W.G. 2001. Sedimentology. 48(2). 255-267.
2. Chepil W.S. 1945. Soil Science. 60(4).305-320.
3. Anderson R.S. 1987. Sedimentology, 34(5), 943-956.
4. Hoyle R.B., Woods A.W. 1997. Physical Review E, 56(6), 6861.
5. Chkhetiani O.G., Gledzer E.B., Artamonova M.S., Iordanskii M.A. Atmospheric Chemistry and Physics. 2012. 12 (11), 5147
6. Gubanova D.P., Chkhetiani O.G., Kuderina T.M., Iordanskii M.A., Obvintsev Y.I. Izvestiya, Atmospheric and Oceanic Physics. 2018. 54 (8), 777-793
7. Shao Y. Physics and Modelling of Wind Erosion. Springer Netherlands, 2009.
8. Liu Y., Fang H., Huang L., and He G. Numerical simulation of the production of three-dimensional sediment dunes. Physics of Fluids,31(9):096603, 2019.
9. Kornev V. M. and Razvorotneva L. I. Comparative estimates of the strength of dry and wet quartz in grinding. Journal of Applied Mechanics and Technical Physics, 39(1):121-126, 1998.
10. Semenov O.E. Introduction to experimental meteorology and climatology of the sand storms, Fizmatkniga, Moscow (in Russian), 2020.